



NMP3 - CT - 2004 - 500311

Sustainpack

Innovation and sustainable Development in the Fibre Based Packaging Value Chain

Instrument: **IP**

D.2.17

Moisture cycling and mechano-sorptive creep

Due date of deliverable: 2005-11-30

Actual submission date: 2006-04-24

Start date of project: **2004-06-01**

Duration: **4 years**

Organisation name of lead contractor for this deliverable:

STFI-Packforsk AB, Stockholm, Sweden

Johan Alfthan, johan.alfthan@stfi.se

Peter Gudmundson, peter@hallf.kth.se

Project co-funded by the European Commission within the Sixth Framework Programme (2002-2006)		
Dissemination Level		
PU	Public	X
PP	Restricted to other programme participants (including the Commission Services)	
RE	Restricted to a group specified by the consortium (including the Commission Services)	
CO	Confidential, only for members of the consortium (including the Commission Services)	

Author:
Johan Alfthan

Title:
**The effect of humidity cycle amplitude on
accelerated tensile creep of paper**

Abstract

The creep of paper is accelerated by moisture cycling, an effect known as mechano-sorptive creep. In this paper the effect of different amplitudes of the moisture content is investigated experimentally and numerically.

Tensile creep tests were made in a climate chamber. Low basis weight isotropic sheets were used in the tests. The moisture content history was measured during each creep test using a balance placed in the climate chamber.

The experimental results are compared to predictions using a theoretical network model. A brief description of the model is given. In the model it is assumed that the anisotropic hygroexpansion of the fibres produces large stresses at the fiber-fiber bonds when moisture changes. The resulting stress state will accelerate creep if the material obeys creep laws that are non-linear in stress. A quite good fit between the theoretical model and the experimental creep curves is obtained.

1 Introduction

Packages of paper often have to withstand loads for a long time, and it is therefore necessary to take creep into consideration in package design. The creep rate generally increases with increasing humidity. Moreover creep is accelerated by humidity variations, so that the creep in a varying humidity is likely to exceed creep at any constant humidity. This effect is known as mechano-sorptive creep. Mechano-sorptive creep has been known for paper since 1972 (Byrd, 1972a,b) and even longer for wood (Armstrong and Kingston, 1960; Armstrong and Christensen, 1961).

There is no generally accepted model for mechano-sorptive creep, but many models and mechanisms have been proposed. It has been suggested that moisture content changes cause hydrogen bond disruption (Gibson, 1965) or create free volume in the material (Padanyi, 1991, 1993), or that dislocations are created by stresses caused by moisture content changes (Hoffmeyer and Davidson, 1989; Hoffmeyer, 1993; Söremark and Fellers, 1993), or combinations of these mechanisms (Haslach, 1994). Phenomenological models that do not take actual micro-mechanisms into account have also been presented (Ranta-Maunus, 1975; Mårtensson, 1994; Urbanik, 1995).

In some recent investigations (Habeger and Coffin, 2000; Alfthan et al., 2002; Alfthan, 2003) it has been suggested that mechano-sorptive creep is an effect of non-linear creep of the material in combination with large transient stresses created during moisture content changes. The stresses are produced by inhomogeneous hygroexpansion in the material caused by moisture gradients, material heterogeneities or both. These stresses are added to the stress state caused by external mechanical loads. This will only cause a redistribution of stresses, while the average remains the same. The creep will then be accelerated if it depends non-linearly on the stresses. The stress state that produces the accelerated creep is transient, as the large stresses relax during creep, and the moisture has to change again to create a new redistribution of stresses. It has been shown that accelerated creep is produced by models based on this mechanism (Habeger and Coffin, 2000; Alfthan et al., 2002; Alfthan, 2003). Results from experiments specifically designed to test the mechanism have been presented (Habeger and Coffin, 2000; Habeger et al., 2001). There is at least qualitative agreement between the models and experiments. The major advantage of this mechanism in comparison to others is that accelerated creep turns out to be a natural consequence of the creep behaviour of the material, and no special mechanism must be introduced to explain mechano-sorptive creep.

The work presented here aims at further comparisons between a previously developed network model (Alfthan, 2003) and experiments, especially the effect of different moisture content cycle amplitudes. The effect of amplitudes has previously been investigated for compressive creep (Fellers and Panek, 2001), and an attempt to model these experiments has been made (Alfthan, 2003). The model predicted a smaller increase in deformation for small amplitudes than was found in the experiments. The purpose of the experiments and modeling presented here is to further examine this discrepancy. The experimental setup was designed to get conditions resembling the assumptions made in the model, i.e. tensile creep and no moisture gradients in the paper. To achieve the latter, the tests are performed on very thin paper, with a basis weight of 17 g/m². The moisture uptake of the paper was measured simultaneously with the creep tests to get input data for the model.

2 Experimental setup

Creep tests in constant and cyclic humidity are made in a climate chamber (Noske-Kaeser KSP 252/70H) using a creep test rig, Fig. 1, that was designed for this purpose. A 25 mm wide strip of paper is clamped in both ends. The distance between the clamps is 149.2 mm when the specimen is mounted. The rig is suspended in one of the clamps from the ceiling of the climate chamber. The other clamp is loaded by weights. The deformation of the paper specimen is measured by two LVDTs (Linear Variable Differential Transducer, Schaevitz MHR 250 MC), fixed to the clamps on each side of the specimen, see Fig. 1. The average of the signals from the two LVDTs is logged on a computer. It is possible to disconnect one LVDT at a time with a switch and thus check the symmetry of the deformation. The LVDT signal during mounting of a specimen is registered and used as a reference when the deformation is calculated.

To be able to calculate the moisture content of the paper, sheets of the paper are simultaneously weighted on a digital laboratory balance (Sartorius BP110S) inside the climate chamber during the creep tests. The balance is shielded from most of the air circulation in the chamber. The weights are logged on the computer. Tests showed that the humidity surrounding the weighted paper is the same as the humidity in the rest of the chamber. The time lag between humidity and weight of the paper is negligible. The humidity in the climate chamber was controlled within a few % RH. Small disturbances in the humidity regulation can be seen in the moisture content curves calculated from the weights.

Isotropic hand sheets, made of unbleached softwood sulphate pulp beaten to SR number 17.1, are used in the creep tests. The basis weight of the sheets is 17 g/m^2 . The low basis weight is used to avoid moisture gradients through the thickness of the paper during the creep tests.

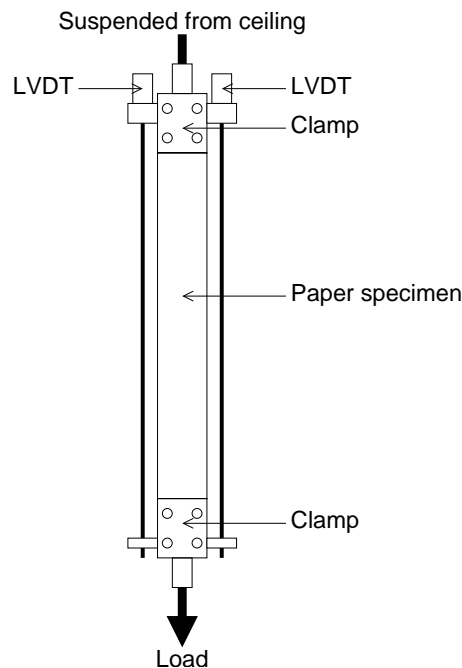


Figure 1. The creep test rig used in the experiments.

3 The network model

Previously a network model for mechano-sorptive creep has been developed (Alfthan, 2003). It resembles Cox's network model for fibrous materials (Cox, 1952), but creep and influence of bonds are added to the model. A brief description of the model is given below.

Each fibre consists of free and bonded sections. The longitudinal strains in the free and bonded sections are denoted ε_A and ε_B respectively. The ratio between the length of the free sections and the total fibre length is denoted λ . The average strain of the fibre is then

$$\varepsilon = \lambda \varepsilon_A + (1 - \lambda) \varepsilon_B. \quad (1)$$

It is assumed that the strain of each fibre is prescribed by the macroscopic strains of the paper sheet. The macroscopic normal strains and shear are denoted as ε_x , ε_y and γ_{xy} where x and y denote coordinates in the plane of the sheet. The strain of a fibre directed in an angle φ from the x -axis then reads

$$\varepsilon = \varepsilon_x \cos^2 \varphi + \varepsilon_y \sin^2 \varphi + \gamma_{xy} \sin \varphi \cos \varphi. \quad (2)$$

Bonded sections of the fibres are assumed to behave as a composite of the fibre itself and the crossing fibre. The transverse strain of the crossing fibre is denoted ε_C and assumed to be equal to the longitudinal strain of the fibre it is bonded to,

$$\varepsilon_C = \varepsilon_B. \quad (3)$$

It is furthermore assumed that the longitudinal load is split between the fibres at the bonds

$$\sigma_A = \sigma_B + \sigma_C, \quad (4)$$

where σ_A and σ_B are the longitudinal stress in the free and bonded segments and σ_C is the transverse stress in the crossing fibre.

The macroscopic stresses in the sheet are the volume averages of the fibre stresses. For paper, specific stresses (stress divided by density) are often used, as it is more convenient to measure the basis weight than the thickness. Averaging over all the fibres leads to the specific stresses

$$\sigma_x^w = \frac{1}{\rho_f} \int_{-\pi/2}^{\pi/2} \sigma_A f(\varphi) \cos^2 \varphi d\varphi \quad (5)$$

$$\sigma_y^w = \frac{1}{\rho_f} \int_{-\pi/2}^{\pi/2} \sigma_A f(\varphi) \sin^2 \varphi d\varphi \quad (6)$$

$$\tau_{xy}^w = \frac{1}{\rho_f} \int_{-\pi/2}^{\pi/2} \sigma_A f(\varphi) \sin \varphi \cos \varphi d\varphi \quad (7)$$

where σ_x^w , σ_y^w and τ_{xy}^w are the specific stresses, ρ_f is the fibre density and $f(\varphi)$ is a frequency function for the fibre distribution in the sheet, which must satisfy

$$\int_{-\pi/2}^{\pi/2} f(\varphi) d\varphi = 1. \quad (8)$$

For an isotropic sheet we have $f(\varphi) = 1/\pi$.

The strains in each fibre segment are assumed to be the sum of elastic strains ε^e , creep strains ε^c and hygroexpansive strains ε^h ,

$$\varepsilon_A = \varepsilon_A^e + \varepsilon_A^c + \varepsilon_A^h, \quad (9)$$

$$\varepsilon_B = \varepsilon_B^e + \varepsilon_B^c + \varepsilon_B^h, \quad (10)$$

$$\varepsilon_C = \varepsilon_C^e + \varepsilon_C^c + \varepsilon_C^h. \quad (11)$$

The elastic strains are assumed to be linear in stresses,

$$\varepsilon_A^e = \sigma_A/E_L, \quad (12)$$

$$\varepsilon_B^e = \sigma_B/E_L, \quad (13)$$

$$\varepsilon_C^e = \sigma_C/E_T, \quad (14)$$

where E_L and E_T are the elastic moduli along and across the fibres, and the hygroexpansive strains are assumed to be proportional to the change in moisture content, Δm ,

$$\varepsilon_A^h = \beta_L \Delta m, \quad (15)$$

$$\varepsilon_B^h = \beta_L \Delta m, \quad (16)$$

$$\varepsilon_C^h = \beta_T \Delta m, \quad (17)$$

where β_L and β_T are the longitudinal and transversal hygroexpansion coefficients. These coefficients are different, and large stresses will therefore be built up when the moisture content changes. In this work, the moisture content m was assumed to be homogeneously distributed in the material, i.e. no moisture gradients are present.

In order to get accelerated creep from the model, the creep strains should obey non-linear creep laws, i.e. the creep rate is given by

$$\dot{\varepsilon}^c = g(\sigma, \varepsilon^c) \quad (18)$$

where g is a non-linear function of stress σ and possibly the creep strain ε^c . In this work the creep rate was modeled as

$$\dot{\varepsilon}_A^c = a_L \sinh(b_L(\sigma_A - E_L^c \varepsilon_A^c)), \quad (19)$$

$$\dot{\varepsilon}_B^c = a_L \sinh(b_L(\sigma_B - E_L^c \varepsilon_B^c)), \quad (20)$$

$$\dot{\varepsilon}_C^c = a_T \sinh(b_T(\sigma_C - E_T^c \varepsilon_C^c)), \quad (21)$$

where a_L , a_T , b_L , b_T , E_L^c and E_T^c are creep parameters. These creep laws will show the necessary non-linearity in stresses and the creep rate will decrease during creep as it does for paper, while the number of parameters remains quite small. Written in a slightly different form, this kind of creep law has been used to model creep of single fibres (Sedlachek, 1995). A problem is that creep will become linear in stresses when the creep strain increases and the arguments of the sinh-functions approach zero, and there will be an ultimate creep limit, $\varepsilon^c = \sigma/E^c$, where the creep stops.

Eqs (1–21) lead to a system of nonlinear ordinary differential equations, which can be solved numerically for strains ε_x , ε_y and γ_{xy} if the stresses σ_x , σ_y and τ_{xy} are known, or the other way around. Details are given in Alfthan (2003).

4 Results

Creep tests are made both in constant humidity, 80 % RH, and in cyclic humidity, cycling from 80 % to 70 %, from 80 % to 60 % and from 80 % to 40 % RH. The temperature was constant at 20°C. The cycle period was 6 h (21600 s), and the humidity changes took 25 minutes (1500 s). The specific stress was 4.9 kNm/kg in the tests presented here. Between 4 and 8 tests were made for each humidity condition, and a few tests were also made for higher loads. Fig. 2 shows some of the experimental creep curves. It is obvious that the creep is accelerated by the humidity changes. Examples of moisture content during these creep tests are shown in Fig. 3.

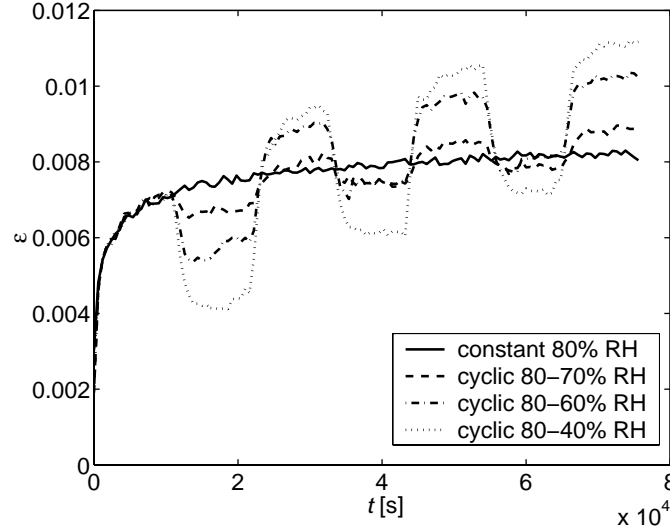


Figure 2. Experimental creep curves for different humidity conditions. The data are filtered to make the plot clearer.

The parameters in the model were fitted to the experiments, using standard MATLAB (2001) routines for the non-linear fit of E_L , a_L , b_L and E_L^c . To reduce the number of necessary parameters to fit, a prescribed ratio r_1 between transverse compliances $1/E_T$, a_T , $1/E_T^c$ and longitudinal compliances $1/E_L$, a_L , $1/E_L^c$ was defined, i.e.

$$\frac{1/E_T}{1/E_L} = \frac{a_T}{a_L} = \frac{1/E_T^c}{1/E_L^c} = r_1. \quad (22)$$

The compliance of paper increases with increasing moisture content. In the model, two moisture contents were chosen, $m = 0.10$ and $m = 0.15$, a ratio r_2 was set between compliances at the high and low moisture content,

$$\frac{1/E_L(m = 0.15)}{1/E_L(m = 0.10)} = \frac{a_L(m = 0.15)}{a_L(m = 0.10)} = \frac{1/E_L^c(m = 0.15)}{1/E_L^c(m = 0.10)} = r_2, \quad (23)$$

and the compliances were assumed to vary linearly between these two values. The parameter b_T was assumed to be equal to b_L . The fit was repeated for a few sets of values for the remaining parameters, until an acceptable fit was obtained. All parameters are presented in Table 1. The results for constant and cyclic humidities are shown in Figs 4–6. Data from individual creep tests, not average curves, are used in the simulations.

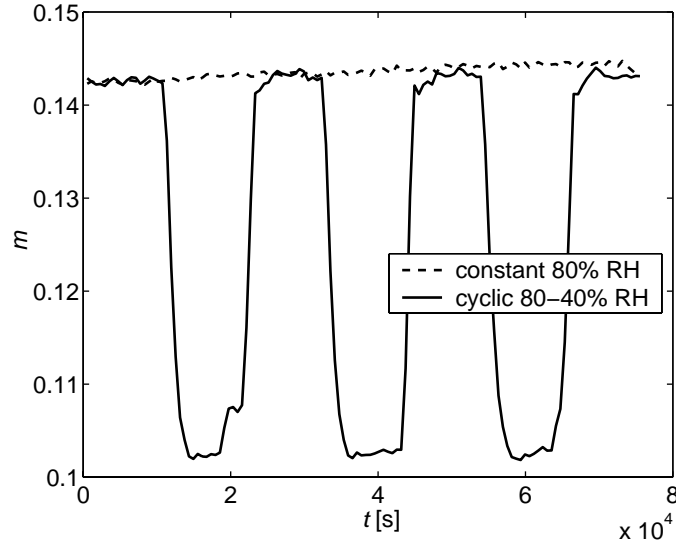


Figure 3. Moisture content for constant 80 % RH and cyclic 80 % to 40 % RH. The data are filtered to make the plot clearer. The slight increase in moisture content for the constant humidity is caused by the humidity regulation of the climate chamber.

Table 1. Parameters used in the network model. Two values are given for moisture dependent parameters.

		moisture content	
		$m = 0.10$	$m = 0.15$
E_L	[GPa]	6.85	4.57
E_T	[GPa]	3.42	2.28
a_L	[s ⁻¹]	$1.77 \cdot 10^{-10}$	$2.66 \cdot 10^{-10}$
a_T	[s ⁻¹]	$8.87 \cdot 10^{-11}$	$1.33 \cdot 10^{-10}$
b_L	[Pa ⁻¹]	$4.99 \cdot 10^{-7}$	
b_T	[Pa ⁻¹]	$4.99 \cdot 10^{-7}$	
E_L^c	[GPa]	2.24	1.50
E_T^c	[GPa]	1.12	0.75
β_L			0.0
β_T			0.6
ρ_f	[kg/m ³]		1500
λ			0.75

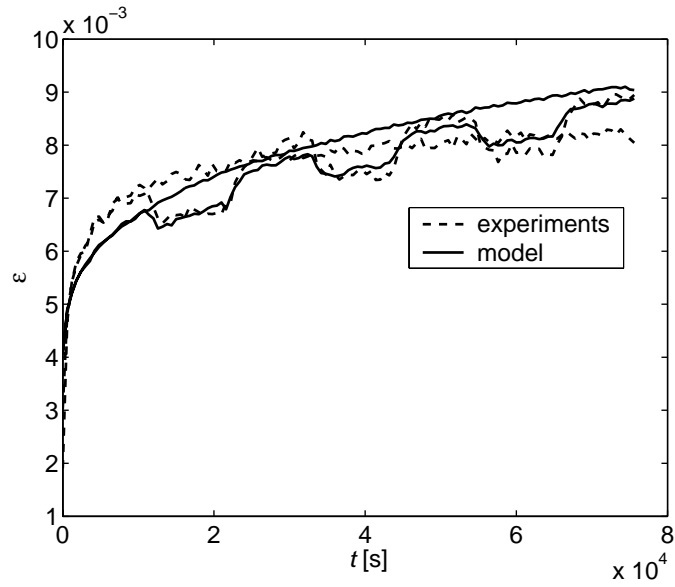


Figure 4. Experimental creep curves for constant 80 % RH and cyclic 80 % to 70 % RH, and corresponding creep curves from the model. The data are filtered to make the plot clearer.

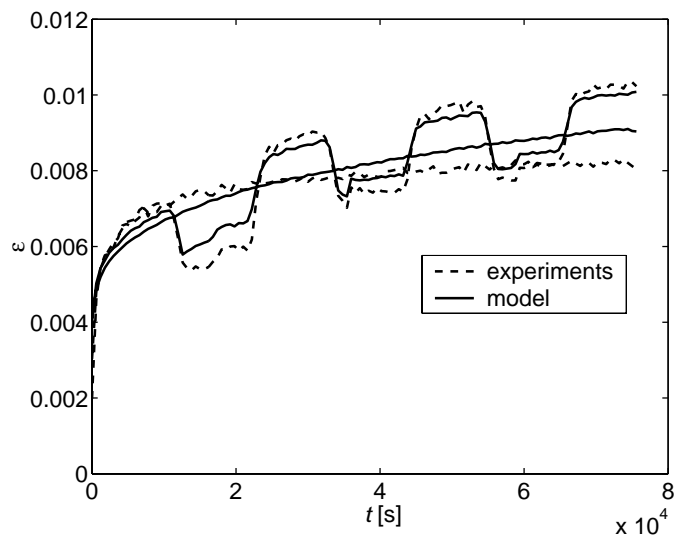


Figure 5. Experimental creep curves for constant 80 % RH and cyclic 80 % to 60 % RH, and corresponding creep curves from the model. The data are filtered to make the plot clearer.

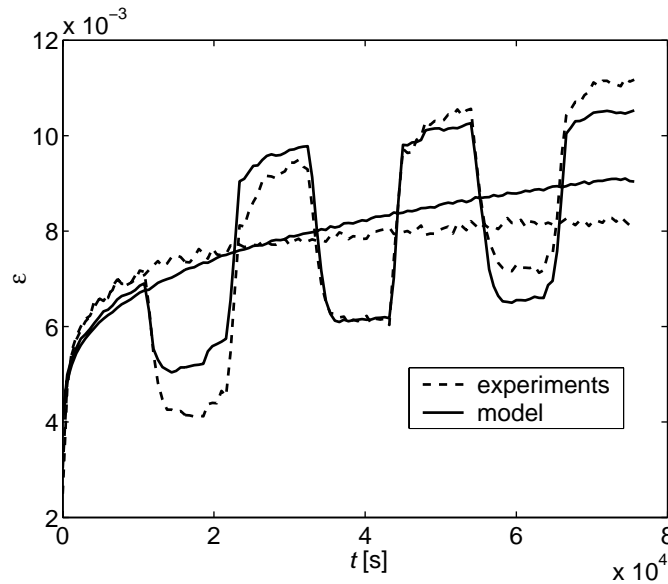


Figure 6. Experimental creep curves for constant 80 % RH and cyclic 80 % to 40 % RH, and corresponding creep curves from the model. The data are filtered to make the plot clearer.

The total strain after the 1st, 2nd and 3rd cycles are shown as a function of moisture content amplitude $|\Delta m|$ in Figs 7–9 for the experiments and the model.

The creep limit $\varepsilon^c = \sigma/E^c$, predicted by the creep laws Eqs (19–21), turned out to be important in the curve fitting. Either the simulated creep curves for cyclic humidity would reach this creep limit too soon or the creep curve for constant humidity would be too steep. The best parameter fit was a compromise, and Fig. 6 shows that the simulated cyclic moisture content creep curve underestimates the actual deformation during the last cycle, while the simulated constant moisture content creep curve is too steep. The compromise also leads to very little accelerated creep for small changes in moisture content, and the mechano-sorptive creep effect is lost in the model as Fig. 4 shows. This is also reflected in Figs 7–9 where the model prediction for deformation at constant humidity is always too high, while the agreement is better for cyclic humidities. The experimental data presented in Figs 7–9 show that a small moisture content amplitude gives a small increase in deformation, intermediate amplitude gives a large increase, and only little additional deformation is obtained if the amplitude is further increased.

5 Conclusions and discussion

From this work it can be concluded that it is possible to get a reasonable fit between simulated and experimental creep curves, and that the model can capture the effect of different amplitudes of the humidity cycles in tensile creep. The model parameters were however not measured independently. One effect of this is the low value of the fibre modulus, which probably is a result of some effects not covered by the model, like bending properties of fibres, shear lag at fibre ends and flaws in the chosen creep law.

The experiments performed in this work or found in the literature are not sufficient for the

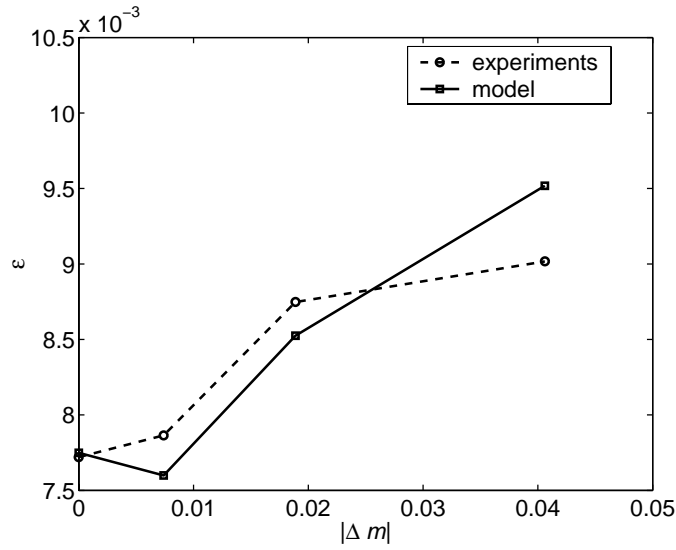


Figure 7. Strain after the 1st cycle as function of moisture content amplitude $|\Delta m|$. The values shown are averages of strains from 25000 s to 29000 s (Centered around 7.5 h).

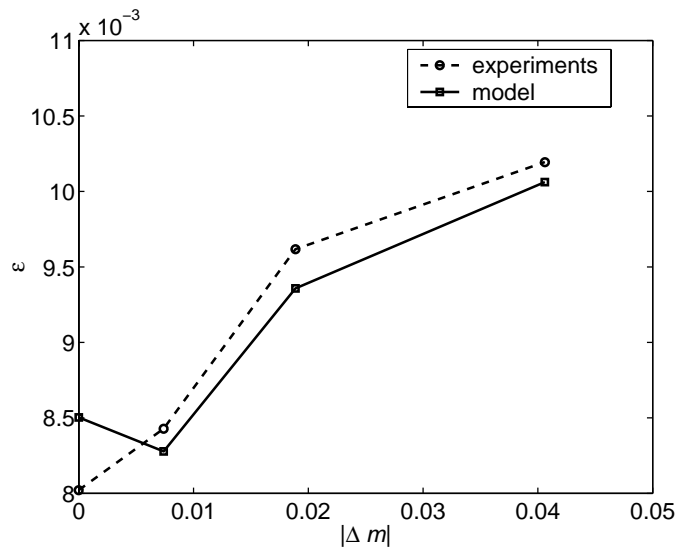


Figure 8. Strain after the 2nd cycle as function of moisture content amplitude $|\Delta m|$. The values shown are averages of strains from 46600 s to 50600 s (Centered around 13.5 h).

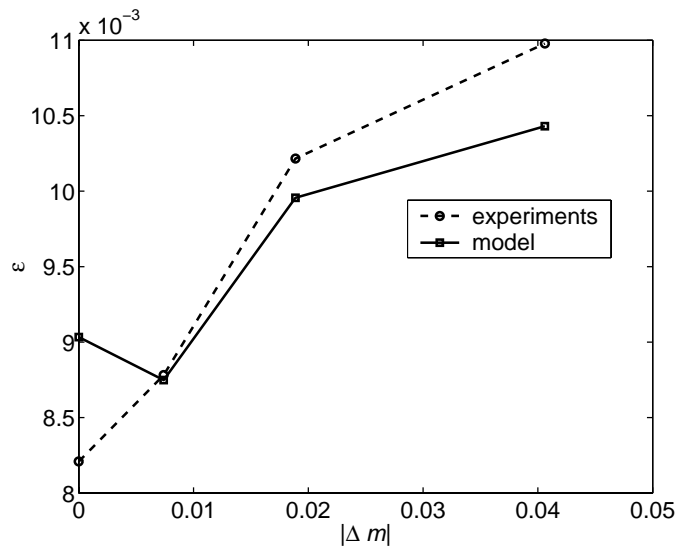


Figure 9. Strain after the 3rd cycle as function of moisture content amplitude $|\Delta m|$. The values shown are averages of strains from 68200 s to 72200 s (Centered around 19.5 h).

development of a model that can be expected to well describe the creep of fibres and paper when the stress varies during the creep test. The creep law is therefore a major weakness of the present model. It was found that it could not describe creep well at different stress levels, and that the ultimate creep limit predicted had a large influence on the simulated creep curves. This was not totally unexpected, as previous work indicates a too fast decrease in creep rate during creep (Alfthan, 2003) and curve fits to creep of single fibres show large variations in parameters (Sedlacek, 1995).

The effect of moisture content cycle amplitude on tensile mechano-sorptive creep differs slightly from the effect that has been found for small amplitude compressive creep (Fellers and Panek, 2001). In the present work it was found that the largest increase in deformation with amplitude was found for intermediate moisture content cycle amplitudes. In the compressive creep tests (Fellers and Panek, 2001), this difference between the smallest and intermediate moisture content amplitudes was not found. However, it is possible that this effect can be found for amplitudes smaller than those tested in Fellers and Panek (2001).

References

- Alfthan, J. (2003). A simplified network model for mechano-sorptive creep in paper. *J. Pulp Paper Sci.*, 29(7):228–234.
- Alfthan, J., Gudmundson, P., and Östlund, S. (2002). A micro-mechanical model for mechano-sorptive creep in paper. *J. Pulp Paper Sci.*, 28(3):98–104.
- Armstrong, L. D. and Christensen, G. N. (1961). Influence of moisture changes on deformation of wood under stress. *Nature*, 191(4791):869–870.

- Armstrong, L. D. and Kingston, R. S. T. (1960). Effect of moisture changes on creep in wood. *Nature*, 185(4718):862–863.
- Byrd, V. L. (1972a). Effect of relative humidity changes during creep on handsheet paper properties. *Tappi*, 55(2):247–252.
- Byrd, V. L. (1972b). Effect of relative humidity changes on compressive creep response of paper. *Tappi*, 55(11):1612–1613.
- Cox, H. L. (1952). The elasticity and strength of paper and other fibrous materials. *Brit. J. Appl. Phys.*, 3:72–79.
- Fellers, C. and Panek, J. (2001). Effect of relative humidity cycling on mechano-sorptive creep. In *Moisture and creep effects on paper, board and containers: 5th international symposium*, Marysville, Victoria, Australia.
- Gibson, E. J. (1965). Creep of wood: Role of water and effect of a changing moisture content. *Nature*, 206(4980):213–215.
- Habeger, C. C. and Coffin, D. W. (2000). The role of stress concentrations in accelerated creep and sorption-induced physical aging. *J. Pulp Paper Sci.*, 26(4):145–157.
- Habeger, C. C., Coffin, D. W., and Hojjatie, B. (2001). Influence of humidity cycling parameters on the moisture-accelerated creep of polymeric fibers. *J. Polym. Sci. Part B Polym. Phys.*, 39(17):2048–2062.
- Haslach, H. W. (1994). The mechanics of moisture accelerated tensile creep in paper. *Tappi J.*, 77(10):179–186.
- Hoffmeyer, P. (1993). Nonlinear creep caused by slip plane formation. *Wood Sci. Technol.*, 27:321–335.
- Hoffmeyer, P. and Davidson, R. W. (1989). Mechano-sorptive creep mechanism of wood in compression and bending. *Wood Sci. Technol.*, 23:215–227.
- Mårtensson, A. (1994). Mechano-sorptive effects in wooden material. *Wood Sci. Technol.*, 28:437–449.
- MATLAB (2001). *MATLAB 6.1*. The MathWorks, Inc., Natick, Massachusetts.
- Padanyi, Z. V. (1991). Mechano-sorptive effects and accelerated creep in paper. In *1991 International Paper Physics Conference*, pages 397–411, Kona, Hawaii.
- Padanyi, Z. V. (1993). Physical aging and glass transition: Effects on the mechanical properties of paper and board. In *Products of Papermaking*, volume 1, pages 521–545, Oxford.
- Ranta-Maunus, A. (1975). The viscoelasticity of wood at varying moisture content. *Wood Sci. Technol.*, 9:189–205.
- Sedlachek, K. M. (1995). *The effect of hemicelluloses and cyclic humidity on the creep of single fibers*. PhD thesis, Institute of Paper Science and Technology, Atlanta, Georgia.

- Söremark, C. and Fellers, C. (1993). Mechano-sorptive creep and hygroexpansion of corrugated board in bending. *J. Pulp Paper Sci.*, 19(1):J19–J26.
- Urbanik, T. J. (1995). Hygroexpansion-creep model for corrugated fiberboard. *Wood Fiber Sci.*, 27(2):134–140.

Authors:

Johan Alfthan and Peter Gudmundson

Title:

**Linear constitutive model for mechano-
sorptive creep in paper**

Abstract

The creep of paper is accelerated by moisture cycling. This effect is known as mechano-sorptive creep. It is assumed that this is an effect of transient stresses produced during moisture content changes in combination with non-linear creep behaviour of the fibres. The stresses produced by the moisture content changes are often much larger than the applied mechanical loads. If this is the case, the mechanical loads are only a perturbation to the internal stress state, and it will appear as if the mechano-sorptive creep is linear in stress. It is possible to take advantage of this feature. In the present report the pure moisture problem is first solved. The mechanical load is then treated as a perturbation of the solution to the moisture problem. Using this strategy, it is possible to linearize a non-linear network model for mechano-sorptive creep and to formulate a continuum model. As a result, the number of variables in the model is reduced. This is a significant improvement as it will be possible to use the linearized model to describe the material in a finite element program and solve problems with complicated geometries.

1 Introduction

Paper and board packages are often loaded for times long enough for creep to be important, and this must be considered in design. Paper is sensitive to moisture and the creep compliance increases with moisture content. High humidity climate is however not the worst possible environment as creep is also accelerated by varying humidity (Byrd, 1972a,b). The accelerated creep is known as mechano-sorptive creep, and is also found in wood (Armstrong and Kingston, 1960; Armstrong and Christensen, 1961), concrete (Pickett, 1942) and some synthetic fibres (Wang et al., 1990, 1991, 1992, 1993; Habeger and Coffin, 2000; Habeger et al., 2001).

There is still no generally accepted explanation for mechano-sorptive creep, but there are several hypotheses and models. One possible explanation is that large local stresses are produced when the moisture content changes due to inhomogeneous hygroexpansion, which in turn will accelerate the creep if the creep rate depends non-linearly on stresses. Models have demonstrated that this mechanism will produce accelerated creep resembling the creep behaviour found in experiments (Pickett, 1942; Habeger and Coffin, 2000; Alfthan et al., 2002; Alfthan, 2003). The advantage over several other models is that no special mechanism is introduced to explain mechano-sorptive creep – it is known that the creep of fibres and paper is non-linear and inhomogeneous hygroexpansion can be the result of material inhomogeneities, moisture gradients or both. However, the non-linearity necessary for the mechanism makes the models complicated, and numerical methods are necessary even for simple problems. The network models (Alfthan et al., 2002; Alfthan, 2003) include many variables and equations to solve, and numerical simulations are therefore very slow.

In Alfthan (2003) it was found that the network model, albeit based on a non-linear mechanism, exhibited an almost linear behaviour between stresses and strains for mechanical loads that are encountered in applications. In the present paper, this feature is exploited to linearize the model, and a continuum model for mechano-sorptive creep of paper with a reduced number of variables is obtained. This linearized model can for example be implemented as a material model in a finite element program and it can be used to solve problems with more complicated geometries, for example a corrugated board container.

2 Linearization of the network model

It is assumed that the internal stresses produced by inhomogeneous hygroexpansion are much larger than the stresses produced by externally applied mechanical loads, and that the latter can be treated as a small perturbation of the former stress

state. An approximate solution to a problem with moisture variations and external loads is then obtained by first solving a non-linear problem with moisture variations but no external loads, and then solve a linearized problem to get the perturbation caused by the external loads. A related analysis of moisture induced transients in DMA response of a simple one dimensional model is found in Coffin and Habeger (2001).

Fig. 1 shows the geometry of a fibre. In the following, index A is used for variables and constants for the free segments, index B is used for the bonded segments and index C is used for the bonded crossing fibres. Properties with index A or B reflect the longitudinal behaviour of fibres, while properties with index C reflect the transverse behaviour.

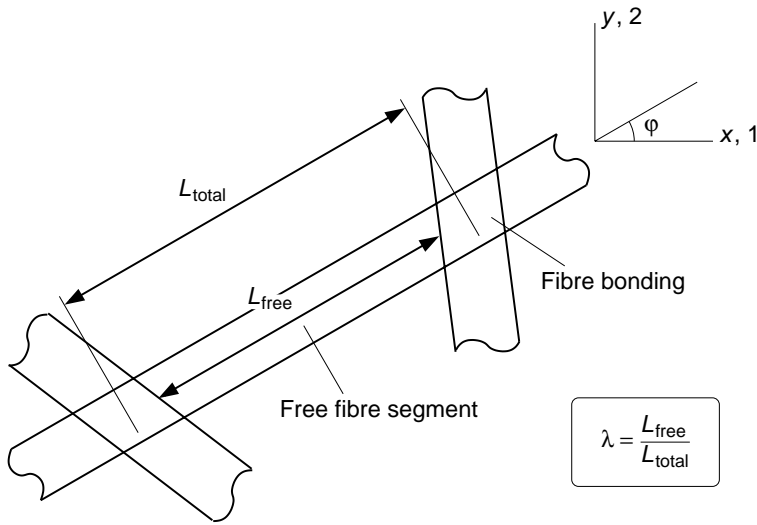


Figure 1. Geometry of the fibre segments. The ratio λ is defined as the length of the free segments, L_{free} , divided by the total length, L_{total} , and the direction of the fibre is defined by the angle ϕ measured from the x -axis of the coordinate system.

2.1 Analysis of the pure moisture problem

First the pure moisture problem is considered. It is assumed that the moisture content m is known as a function of time t , $m = m(t)$. It is also assumed that the free segments of the fibres can expand freely so that no stresses are created, i.e.

$$\varepsilon_A = \beta_A m, \quad (1)$$

$$\sigma_A = 0. \quad (2)$$

For the bonded segments, see Fig. 1, strains and stresses are related by

$$\varepsilon_B = \varepsilon_C, \quad (3)$$

$$\sigma_B + \sigma_C = 0. \quad (4)$$

where it has been assumed that fibres cross at right angles. The stresses σ_B and σ_C relax as the material creeps and will eventually vanish. The constitutive laws for the bonded fibre segments read

$$\varepsilon_B = \frac{\sigma_B}{E_B} + \varepsilon_B^c + \beta_B m, \quad (5)$$

$$\varepsilon_C = \frac{\sigma_C}{E_C} + \varepsilon_C^c + \beta_C m, \quad (6)$$

where the creep strains ε_B^c and ε_C^c are given by the creep laws

$$\dot{\varepsilon}_B^c = f_B(\sigma_B, \varepsilon_B^c), \quad (7)$$

$$\dot{\varepsilon}_C^c = f_C(\sigma_C, \varepsilon_C^c). \quad (8)$$

For a given moisture content history, Eqs (1–8) constitute a non-linear system of equations for the stresses and strains of the pure moisture problem.

The average strain of a fibre will be

$$\varepsilon = \lambda \varepsilon_A + (1 - \lambda) \varepsilon_B, \quad (9)$$

where λ is the ratio between free fibre length and total fibre length, see Fig. 1. For an anisotropic fibre orientation, the ratio λ generally vary with orientation.

The average strain is also related to the macroscopic strains of the sheet. In accordance with Alfthan (2003), it is assumed that the strain of a fibre is equal to the macroscopic strain in the fibre direction, i.e.

$$\varepsilon = \varepsilon_x \cos^2 \varphi + \varepsilon_y \sin^2 \varphi + \gamma_{xy} \sin \varphi \cos \varphi, \quad (10)$$

where φ is the angle of the fibre measured from the x -axis.

If the fibre distribution is given, it is possible to calculate the number of fibre crossings (Komori and Makishima, 1977), and from that the ratio λ can be calculated. For a plane fibre network, with rectangular cross sections of the fibres, the ratio λ is given by

$$\lambda = 1 - 2\rho \int_{-\pi/2}^{\pi/2} f(\psi) |\sin(\varphi - \psi)| d\psi \quad (11)$$

where f is the frequency function of the fibre distribution. If the frequency function is

$$f = \frac{1}{\pi} (1 + \alpha \cos 2\varphi), \quad (12)$$

then λ will be given by

$$\lambda = \lambda_x \cos^2 \varphi + \lambda_y \sin^2 \varphi, \quad (13)$$

with

$$\lambda_x = 1 - \frac{4\rho}{\pi} + \frac{4\rho\alpha}{3\pi}, \quad (14)$$

$$\lambda_y = 1 - \frac{4\rho}{\pi} - \frac{4\rho\alpha}{3\pi}, \quad (15)$$

where ρ is the volume fraction of fibres in the network.

In this case the initial assumptions Eqs (1–2) will be fulfilled, and Eqs (9–10) will be reduced to

$$\varepsilon_x = \lambda_x \varepsilon_A + (1 - \lambda_x) \varepsilon_B, \quad (16)$$

$$\varepsilon_y = \lambda_y \varepsilon_A + (1 - \lambda_y) \varepsilon_B, \quad (17)$$

$$\gamma_{xy} = 0. \quad (18)$$

For general fibre distributions, Eqs (1–2) will not be exactly satisfied, but the error is quite small.

2.2 Linearized analysis of the mechanical problem

In the following analysis, it is assumed that the mechanical load can be treated as a small perturbation to the moisture problem. The perturbation strains $\delta\varepsilon_A$, $\delta\varepsilon_B$ and $\delta\varepsilon_C$ in a fibre are then given by

$$\delta\varepsilon_A = \frac{\delta\sigma_A}{E_A} + \delta\varepsilon_A^c, \quad (19)$$

$$\delta\varepsilon_B = \frac{\delta\sigma_B}{E_B} + \delta\varepsilon_B^c, \quad (20)$$

$$\delta\varepsilon_C = \frac{\delta\sigma_C}{E_C} + \delta\varepsilon_C^c, \quad (21)$$

where $\delta\sigma_A$, $\delta\sigma_B$ and $\delta\sigma_C$ are the perturbations in stress and $\delta\varepsilon_A^c$, $\delta\varepsilon_B^c$ and $\delta\varepsilon_C^c$ are the creep strains caused by the perturbation.

The creep strains will be given by Eqs (7–8) and the corresponding creep law for the free segments,

$$\dot{\varepsilon}_A^c = f_A(\sigma_A, \varepsilon_A^c). \quad (22)$$

The functions f_A and f_B are equal as both are used to describe the longitudinal behaviour of the fibres.

The mechanical stresses are only a perturbation to the stress state of the pure moisture problem, so it is viable to approximate the creep laws by Taylor expansions,

$$\dot{\varepsilon}_A^c \approx f_A(0,0) + \frac{\partial f_A}{\partial \sigma_A}(0,0)\delta\sigma_A + \frac{\partial f_A}{\partial \varepsilon_A^c}(0,0)\delta\varepsilon_A^c, \quad (23)$$

$$\dot{\varepsilon}_B^c \approx f_B(\sigma_B^0, \varepsilon_B^{c0}) + \frac{\partial f_B}{\partial \sigma_B}(\sigma_B^0, \varepsilon_B^{c0})\delta\sigma_B + \frac{\partial f_B}{\partial \varepsilon_B^c}(\sigma_B^0, \varepsilon_B^{c0})\delta\varepsilon_B^c, \quad (24)$$

$$\dot{\varepsilon}_C^c \approx f_C(\sigma_C^0, \varepsilon_C^{c0}) + \frac{\partial f_C}{\partial \sigma_C}(\sigma_C^0, \varepsilon_C^{c0})\delta\sigma_C + \frac{\partial f_C}{\partial \varepsilon_C^c}(\sigma_C^0, \varepsilon_C^{c0})\delta\varepsilon_C^c, \quad (25)$$

where σ_B^0 , ε_B^{c0} , σ_C^0 and ε_C^{c0} are the time dependent stresses and strains that result from the pure moisture problem. Identification of the perturbations to the creep strain rates, $\delta\dot{\varepsilon}_A^c$, $\delta\dot{\varepsilon}_B^c$ and $\delta\dot{\varepsilon}_C^c$, leads to the linearized creep laws

$$\delta\dot{\varepsilon}_A^c = \frac{\partial f_A}{\partial \sigma_A}(0,0)\delta\sigma_A + \frac{\partial f_A}{\partial \varepsilon_A^c}(0,0)\delta\varepsilon_A^c, \quad (26)$$

$$\delta\dot{\varepsilon}_B^c = \frac{\partial f_B}{\partial \sigma_B}(\sigma_B^0, \varepsilon_B^{c0})\delta\sigma_B + \frac{\partial f_B}{\partial \varepsilon_B^c}(\sigma_B^0, \varepsilon_B^{c0})\delta\varepsilon_B^c, \quad (27)$$

$$\delta\dot{\varepsilon}_C^c = \frac{\partial f_C}{\partial \sigma_C}(\sigma_C^0, \varepsilon_C^{c0})\delta\sigma_C + \frac{\partial f_C}{\partial \varepsilon_C^c}(\sigma_C^0, \varepsilon_C^{c0})\delta\varepsilon_C^c. \quad (28)$$

The perturbation strains and stresses in the fibre are related by

$$\delta\varepsilon_B = \delta\varepsilon_C, \quad (29)$$

$$\delta\sigma_B + \delta\sigma_C = \delta\sigma_A = \delta\sigma, \quad (30)$$

$$\delta\varepsilon = \lambda\delta\varepsilon_A + (1-\lambda)\delta\varepsilon_B, \quad (31)$$

where $\delta\sigma$ has been introduced as a shorthand for the stress in the free segments.

Eqs (19–31) can be interpreted as a linear rheological model, see Fig. 2. The parameters of the rheological model are identified from Eqs (26–28),

$$\frac{1}{\eta_A} = \frac{\partial f_A}{\partial \sigma_A}(0,0), \quad (32)$$

$$\frac{1}{E_A^2} = -\frac{\partial f_A}{\partial \sigma_A}(0,0) / \frac{\partial f_A}{\partial \varepsilon_A^c}(0,0), \quad (33)$$

$$\frac{1}{\eta_B} = \frac{\partial f_B}{\partial \sigma_B}(\sigma_B^0, \varepsilon_B^{c0}), \quad (34)$$

$$\frac{1}{E_B^2} = -\frac{\partial f_B}{\partial \sigma_B}(\sigma_B^0, \varepsilon_B^{c0}) / \frac{\partial f_B}{\partial \varepsilon_B^c}(\sigma_B^0, \varepsilon_B^{c0}), \quad (35)$$

$$\frac{1}{\eta_C} = \frac{\partial f_C}{\partial \sigma_C}(\sigma_C^0, \varepsilon_C^{c0}), \quad (36)$$

$$\frac{1}{E_C^2} = -\frac{\partial f_C}{\partial \sigma_C}(\sigma_C^0, \varepsilon_C^{c0}) / \frac{\partial f_C}{\partial \varepsilon_C^c}(\sigma_C^0, \varepsilon_C^{c0}). \quad (37)$$

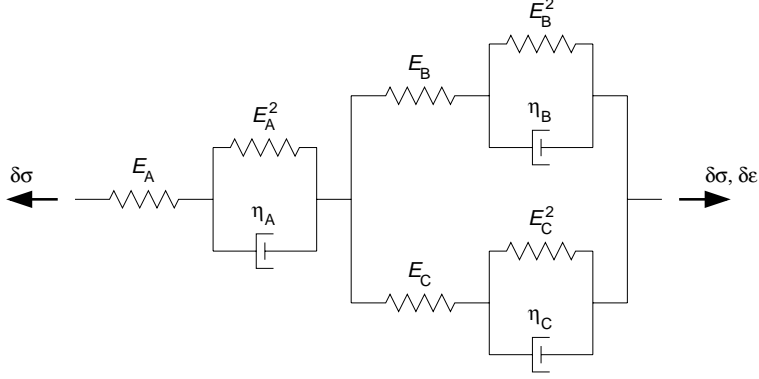


Figure 2. A rheological model representing Eqs (19–28). The parameters of the rheological model are given by Eqs (32–37).

The parameters depend on the solution from the pure moisture problem, hence they will be time dependent. Using the parameters of the rheological model, Eqs (26–28) can be rewritten as

$$\delta \varepsilon_A^c = \frac{\delta \sigma_A - E_A^2 \delta \varepsilon_A^c}{\eta_A}, \quad (38)$$

$$\delta \varepsilon_B^c = \frac{\delta \sigma_B - E_B^2 \delta \varepsilon_B^c}{\eta_B}, \quad (39)$$

$$\delta \varepsilon_C^c = \frac{\delta \sigma_C - E_C^2 \delta \varepsilon_C^c}{\eta_C}. \quad (40)$$

If it is assumed that the creep can be described by the non-linear creep laws

$$f_A = a_A \sinh(b_A(\sigma_A - E_A^c \varepsilon_A^c)), \quad (41)$$

$$f_B = a_B \sinh(b_B(\sigma_B - E_B^c \varepsilon_B^c)), \quad (42)$$

$$f_C = a_C \sinh(b_C(\sigma_C - E_C^c \varepsilon_C^c)), \quad (43)$$

then

$$\frac{1}{\eta_A} = a_A b_A, \quad (44)$$

$$E_A^2 = E_A^c, \quad (45)$$

$$\frac{1}{\eta_B} = a_B b_B \cosh(b_B(\sigma_B^0 - E_B^c \varepsilon_B^{c0})), \quad (46)$$

$$E_B^2 = E_B^c, \quad (47)$$

$$\frac{1}{\eta_C} = a_C b_C \cosh(b_C(\sigma_C^0 - E_C^c \varepsilon_C^{c0})), \quad (48)$$

$$E_C^2 = E_C^c, \quad (49)$$

where it has been utilized that stresses in the free segments vanish for the moisture problem.

2.3 Continuum model

In this subsection indices i, j, k and l denoted coordinate directions, and they take values 1 and 2 corresponding to x and y respectively, see Fig. 1. A repeated index letter in an expression indicates a sum over that index from 1 to 2. Using this notation, the strain of any fibre is assumed to be given by the macroscopic strains of the sheet according to

$$\delta \varepsilon = \delta \varepsilon_{kl} n_k n_l \quad (50)$$

where $n_1 = \cos \varphi$ and $n_2 = \sin \varphi$, and the macroscopic specific stresses are given by

$$\delta \sigma_{ij}^w = \frac{1}{\rho_f} \int_{-\pi/2}^{\pi/2} \delta \sigma f(\varphi) n_i n_j d\varphi, \quad (51)$$

where ρ_f is the fibre density and $f(\varphi)$ is the frequency function of the fibre distribution, which must fulfill the condition

$$\int_{-\pi/2}^{\pi/2} f(\varphi) d\varphi = 1. \quad (52)$$

Eq. (51) can alternatively be expressed in terms of the operator I_{ij} according to

$$I_{ij}(\chi) = \frac{1}{\rho_f} \int_{-\pi/2}^{\pi/2} \chi f(\varphi) n_i n_j d\varphi, \quad (53)$$

where χ is any function of φ , so that Eq. (51) can be written

$$\delta \sigma_{ij}^w = I_{ij}(\delta \sigma). \quad (54)$$

Applying the operator I_{ij} on $\delta \varepsilon$ according to Eq. (50) results in

$$I_{ij}(\delta \varepsilon) = \frac{1}{\rho_f} \int_{-\pi/2}^{\pi/2} \delta \varepsilon_{kl} f(\varphi) n_i n_j n_k n_l d\varphi = \frac{1}{\rho_f} C_{ijkl} \delta \varepsilon_{kl}, \quad (55)$$

where

$$C_{ijkl} = \int_{-\pi/2}^{\pi/2} f(\varphi) n_i n_j n_k n_l d\varphi. \quad (56)$$

Eqs (54–55) can be written in vector form,

$$\delta \boldsymbol{\sigma}^w = \mathbf{I}(\delta \boldsymbol{\sigma}), \quad (57)$$

$$\mathbf{I}(\delta \boldsymbol{\varepsilon}) = \frac{1}{\rho_f} \mathbf{C} \delta \boldsymbol{\varepsilon} \quad (58)$$

where

$$\delta \boldsymbol{\sigma}^w = \begin{bmatrix} \delta \sigma_{11}^w \\ \delta \sigma_{22}^w \\ \delta \sigma_{12}^w \end{bmatrix} = \begin{bmatrix} \delta \sigma_x^w \\ \delta \sigma_y^w \\ \delta \tau_{xy}^w \end{bmatrix}, \quad (59)$$

$$\delta \boldsymbol{\varepsilon} = \begin{bmatrix} \delta \varepsilon_{11} \\ \delta \varepsilon_{22} \\ 2\delta \varepsilon_{12} \end{bmatrix} = \begin{bmatrix} \delta \varepsilon_x \\ \delta \varepsilon_y \\ \delta \gamma_{xy} \end{bmatrix}, \quad (60)$$

$$\mathbf{C} = \begin{bmatrix} C_{1111} & C_{1122} & C_{1112} \\ C_{2211} & C_{2222} & C_{2212} \\ C_{1211} & C_{1222} & C_{1212} \end{bmatrix}. \quad (61)$$

The operator I_{ij} can as well be applied to Eqs (19–21), Eqs (38–40) and Eqs (29–31), resulting in the corresponding equations

$$\delta \boldsymbol{\varepsilon}_A = \frac{\delta \boldsymbol{\sigma}_A}{E_A} + \delta \boldsymbol{\varepsilon}_A^c, \quad (62)$$

$$\delta \boldsymbol{\varepsilon}_B = \frac{\delta \boldsymbol{\sigma}_B}{E_B} + \delta \boldsymbol{\varepsilon}_B^c, \quad (63)$$

$$\delta \boldsymbol{\varepsilon}_C = \frac{\delta \boldsymbol{\sigma}_C}{E_C} + \delta \boldsymbol{\varepsilon}_C^c, \quad (64)$$

$$\delta \dot{\boldsymbol{\varepsilon}}_A^c = \frac{\delta \boldsymbol{\sigma}_A - E_A^2 \delta \boldsymbol{\varepsilon}_A^c}{\eta_A}, \quad (65)$$

$$\delta \dot{\boldsymbol{\varepsilon}}_B^c = \frac{\delta \boldsymbol{\sigma}_B - E_B^2 \delta \boldsymbol{\varepsilon}_B^c}{\eta_B}, \quad (66)$$

$$\delta \dot{\boldsymbol{\varepsilon}}_C^c = \frac{\delta \boldsymbol{\sigma}_C - E_C^2 \delta \boldsymbol{\varepsilon}_C^c}{\eta_C}, \quad (67)$$

$$\delta \boldsymbol{\varepsilon}_B = \delta \boldsymbol{\varepsilon}_C, \quad (68)$$

$$\delta \boldsymbol{\sigma}_B + \delta \boldsymbol{\sigma}_C = \delta \boldsymbol{\sigma}_A = \delta \boldsymbol{\sigma}^w, \quad (69)$$

$$\frac{1}{\rho_f} \mathbf{C} \delta \boldsymbol{\varepsilon} = \mathbf{I}(\lambda \delta \boldsymbol{\varepsilon}_A) + \mathbf{I}((1 - \lambda) \delta \boldsymbol{\varepsilon}_B). \quad (70)$$

Eq. (70) contains the unevaluated expressions $\mathbf{I}(\lambda \delta \boldsymbol{\varepsilon}_A)$ and $\mathbf{I}((1 - \lambda) \delta \boldsymbol{\varepsilon}_B)$. If λ is a constant these will be reduced to $\lambda \delta \boldsymbol{\varepsilon}_A$ and $(1 - \lambda) \delta \boldsymbol{\varepsilon}_B$, but λ is in general a function of φ . It is however possible to evaluate the expressions if it is assumed that $\delta \boldsymbol{\varepsilon}_A$ and $\delta \boldsymbol{\varepsilon}_B$ can be written as

$$\delta \boldsymbol{\varepsilon}_A = q_{Akl} n_k n_l, \quad (71)$$

$$\delta \boldsymbol{\varepsilon}_B = q_{Bkl} n_k n_l, \quad (72)$$

so that

$$\delta \boldsymbol{\varepsilon}_A = \frac{1}{\rho_f} \mathbf{C} \mathbf{q}_A, \quad (73)$$

$$\delta \boldsymbol{\varepsilon}_B = \frac{1}{\rho_f} \mathbf{C} \mathbf{q}_B. \quad (74)$$

In this case Eq. (70) can be written as

$$\frac{1}{\rho_f} \mathbf{C} \delta \boldsymbol{\varepsilon} = \mathbf{L} \mathbf{C}^{-1} \delta \boldsymbol{\varepsilon}_A + (\mathbf{C} - \mathbf{L}) \mathbf{C}^{-1} \delta \boldsymbol{\varepsilon}_B, \quad (75)$$

where

$$\mathbf{L} = \begin{bmatrix} L_{1111} & L_{1122} & L_{1112} \\ L_{2211} & L_{2222} & L_{2212} \\ L_{1211} & L_{1222} & L_{1212} \end{bmatrix}, \quad (76)$$

$$L_{ijkl} = \int_{-\pi/2}^{\pi/2} f(\varphi) \lambda(\varphi) n_i n_j n_k n_l d\varphi. \quad (77)$$

The authors were not able to prove that Eq. (75) is a valid expression in general, but numerical simulations suggest that Eqs (71–72) and Eq. (75) are true.

If the frequency function f is given by Eq. (12) and the length ratio λ is given by Eq. (13), then the the matrices \mathbf{C} and \mathbf{L} will be

$$\mathbf{C} = \frac{1}{8} \begin{bmatrix} 3 + 2\alpha & 1 & 0 \\ 1 & 3 - 2\alpha & 0 \\ 0 & 0 & 1 \end{bmatrix} \quad (78)$$

and

$$\mathbf{L} = \frac{\lambda_x}{64} \begin{bmatrix} 20 + 15\alpha & 4 + \alpha & 0 \\ 4 + \alpha & 4 - \alpha & 0 \\ 0 & 0 & 4 + \alpha \end{bmatrix} + \frac{\lambda_y}{64} \begin{bmatrix} 4 + \alpha & 4 - \alpha & 0 \\ 4 - \alpha & 20 - 15\alpha & 0 \\ 0 & 0 & 4 - \alpha \end{bmatrix}. \quad (79)$$

Eqs (62–69) and Eq. (75) constitute a linear system of differential equations. Most of the variables, $\delta\boldsymbol{\varepsilon}_A$, $\delta\boldsymbol{\varepsilon}_B$, $\delta\boldsymbol{\varepsilon}_C$, $\delta\boldsymbol{\varepsilon}_A^c$, $\delta\boldsymbol{\varepsilon}_B^c$, $\delta\boldsymbol{\varepsilon}_C^c$, $\delta\boldsymbol{\sigma}_B$ and $\delta\boldsymbol{\sigma}_C$, can be regarded as internal variables that can be eliminated, leaving only the applied macroscopic stresses $\delta\boldsymbol{\sigma}^w$ and the resulting macroscopic strains $\delta\boldsymbol{\varepsilon}$. The total strains are obtained by adding $\delta\boldsymbol{\varepsilon}$ to the strains from the moisture problem, Eqs (16–18).

3 Results

In the results presented here, Eq. (12) and Eq. (13) with λ_x and λ_y according to Eqs (14–15) have been used to describe the fibre and bond distributions. The creep of the fibres are assumed to be described by Eqs (41–43). The pure moisture problem, Eqs (1–8), and the mechanical problem, Eqs (62–69) and Eq. (75), were solved in MATLAB (2001), using standard routines for solving the differential equations.

The fibre properties depend on the moisture content. This is reflected by letting the compliances $1/E_A$, $1/E_B$, $1/E_C$, a_A , a_B , a_C , $1/E_A^c$, $1/E_B^c$ and $1/E_C^c$ increase linearly with moisture m , e.g.

$$a_A = a_A(m_1) + \frac{a_A(m_2) - a_A(m_1)}{m_2 - m_1}(m - m_1), \quad (80)$$

where m_1 and m_2 are used as reference points. They were here chosen to be 0.075 and 0.15, respectively. In the simulations, moisture content was initially 0.10, then decreased to 0.05, increased back to 0.10 etcetera. The parameters used in the simulations are shown in Table 1. The time is normalized by the cycle period T , which should be around 5 h for the parameters to be reasonable. Unless stated otherwise the fibre distribution is uniform, i.e. $\alpha = 0$ in Eq. (12).

Fig. 3 shows the total strains for different uniaxial loads, ranging from 3.3 kNm/kg to 13.3 kNm/kg. The agreement between the linearized model and the non-linear network model from Alfthan (2003) is excellent for small loads. For higher loads the agreement gets worse, as the applied load is no longer small compared to the stress state resulting from the pure moisture problem, Fig. 4.

If Eqs (19–31) are interpreted as the linear rheological model in Fig. 2, the accelerated creep seen in Fig. 3 can be interpreted as a result of transient decreases in effective viscosities every time the moisture content changes. Fig. 5 shows that the inverse viscosities $1/\eta_B$ and $1/\eta_C$ have transient peaks whenever the moisture changes.

Figs 6–7 show creep curves for different anisotropy, demonstrating the validity of Eq. (75). Fig. 6 shows uniaxial load and Fig. 7 shows a combination of uniaxial and biaxial load.

Table 1. Parameters used in the simulations. Two values are given for moisture dependent parameters. The creep compliances are normalized by the moisture cycle period T .

		moisture content	
		$m = 0.075$	$m = 0.15$
$E_A = E_B$	[GPa]	32.0	21.3
E_C	[GPa]	6.40	4.27
$Ta_A = Ta_B$		$5.00 \cdot 10^{-6}$	$7.50 \cdot 10^{-6}$
Ta_C		$25.0 \cdot 10^{-6}$	$37.5 \cdot 10^{-6}$
$b_A = b_B$	[Pa ⁻¹]	$1.00 \cdot 10^{-7}$	
b_C	[Pa ⁻¹]	$1.00 \cdot 10^{-7}$	
$E_A^c = E_B^c$	[GPa]	4.00	2.67
E_C^c	[GPa]	0.800	0.533
$\beta_A = \beta_B$		0.030	
β_C		0.60	
ρ		0.50	
ρ_f	[kg/m ³]	1500	

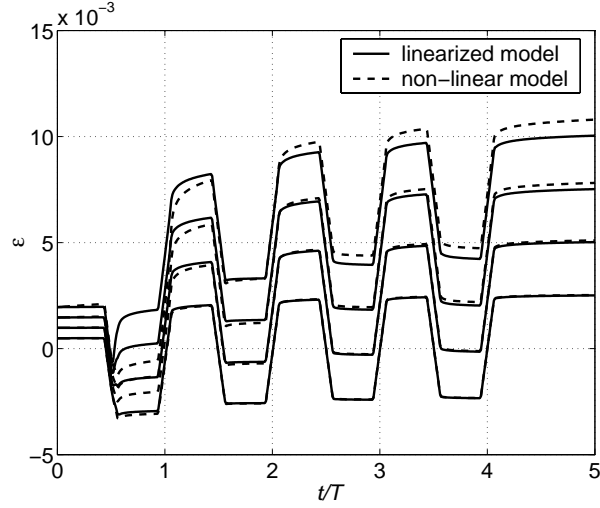


Figure 3. Comparison between the linearized model and the full non-linear network model for different uniaxial loads. The specific stresses are 3.3 (bottom), 6.7, 10.0 and 13.3 kNm/kg (top). The agreement is excellent for small loads, but it gets worse for higher loads as the assumption behind the linearization is no longer valid.

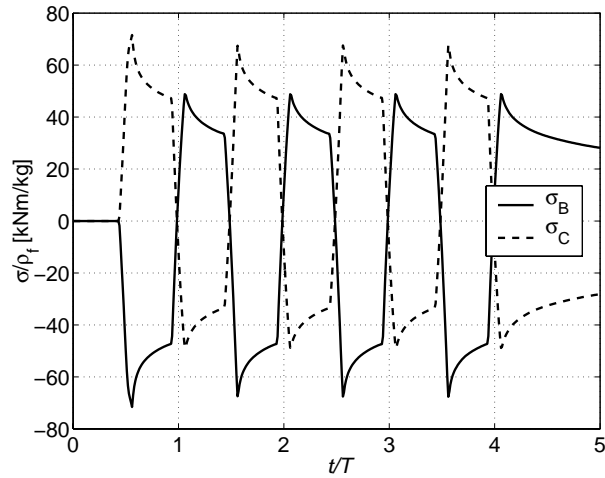


Figure 4. The inner stresses produced by the pure moisture problem. The stresses are divided by fibre density ρ_f so it is possible to compare them to the applied loads. The two curves show the stresses in the two different fibres at the bonds.

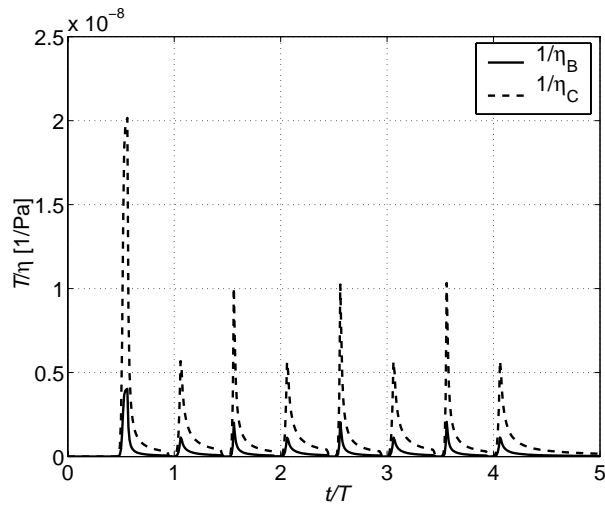


Figure 5. The inverse viscosities $1/\eta_B$ and $1/\eta_C$ as functions of time. The effective viscosities at the bonds, η_B and η_C , are reduced every time the moisture changes resulting in the peaks shown in the plot. Due to the anisotropy of the fibres, η_C is always lower than η_B and the highest peaks corresponds to $1/\eta_C$.

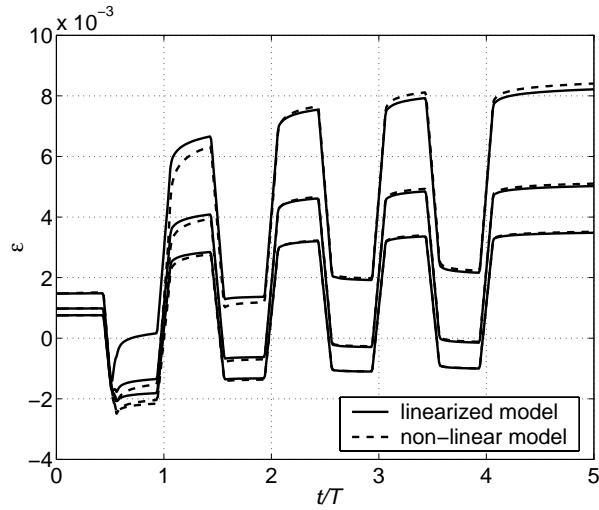


Figure 6. Comparison between the linearized model and the full non-linear network model for different anisotropy. The load is uniaxial. The constant α in Eq. (12) is equal to -0.5 (top), 0 , and $+0.5$ (bottom), and the specific stress is 6.7 kNm/kg .

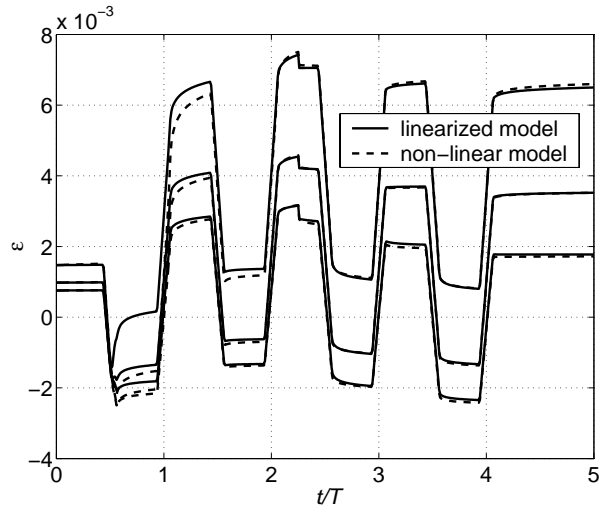


Figure 7. Comparison between the linearized model and the full non-linear network model for different anisotropy. The load is initially uniaxial, but changes to a biaxial load at time $t/T = 2.25$. The constant α in Eq. (12) is equal to -0.5 (top), 0 , and $+0.5$ (bottom), and the specific stresses are 6.7 kNm/kg .

4 Conclusions and discussion

From the results it can be concluded that the agreement between the linearized model and the non-linear network-model is very good for small mechanical loads, as expected from the assumptions made in the linearization. This corresponds to the linear mechano-sorptive creep behaviour often found in experiments, see for example Panek et al. (2004). The linearized model is typically valid when the mechanical load is one order of magnitude smaller than the stresses produced by the moisture changes alone (Fig. 4). For higher loads the linearized model deviates more and more from the non-linear network model.

The major improvement achieved by the linearization and development of a continuum model is the speed of calculations. In the non-linear network model (Alfthan, 2003) a non-linear system of differential equations was solved for three variables in each fibre direction used in the discretization of the fibre distribution. The linearization reduces the model to a small non-linear pure moisture problem of only two variables and a linear mechanical problem. In the continuum formulation, the number of variables of the mechanical problem are reduced, so that only nine linear differential equations remain. In total, eleven differential equations must be solved, and of these only two are non-linear. No discretization of the fibre distribution is necessary. In comparison, 54 non-linear differential equations were solved for each result from the network model shown in Fig. 3 and Figs 6–7. The new model is suitable for implementation as a material model in a finite element code used for solving structural problems, like corrugated board panels or containers subjected to varying humidity and mechanical loads. In Appendix A, an implementation of the model as a user subroutine in ABAQUS (2002) is presented. The finite element formulation has been verified by comparison to MATLAB-calculations described above.

The largest problem with the model is to determine how to describe the creep, as the creep of paper and fibres is not a well-known phenomenon. Here the creep laws are assumed to have the form Eqs (41–43), and parameters were chosen to get results from the simulations that resemble the creep seen in experiments. In practice it is hard to determine the parameters in these creep laws, and it is likely that other creep laws must be adopted to get an accurate description of the creep.

Appendix A Formulation for finite element analysis

In this appendix equations for finite element analysis are formulated. These equations are suitable for two dimensional solid elements or structural elements, like shells. In the following, g_t will denote a variable g at time t , and Δg will be the change of that variable over a time increment Δt . The increment will begin at time t and end at time $t + \Delta t$. A stable time integration scheme will be obtained if central difference operators are adopted, i.e.

$$\dot{g}_{t+\frac{1}{2}\Delta t} = \frac{\Delta g}{\Delta t}, \quad (81)$$

$$g_{t+\frac{1}{2}\Delta t} = g_t + \frac{1}{2}\Delta g. \quad (82)$$

In the commercial finite element program ABAQUS (2002) it is possible for users to define their own constitutive material models in the subroutine UMAT. In the subroutine the material Jacobian matrix, $\partial\Delta\boldsymbol{\sigma}/\partial\Delta\boldsymbol{\varepsilon}$, must be provided for the constitutive model, and stresses and inner state variables must be updated. The equations needed for the implementation of the model will be given below.

A.1 The pure moisture problem

In the pure moisture problem, there are two inner state variables that must be updated, ε_B^c and ε_C^c . These are given by the creep laws Eqs (7–8), in discrete form

$$\frac{\Delta\varepsilon_B^c}{\Delta t} = f_B\left(\sigma_{Bt+\frac{1}{2}\Delta t}, \varepsilon_{Bt+\frac{1}{2}\Delta t}^c\right), \quad (83)$$

$$\frac{\Delta\varepsilon_C^c}{\Delta t} = f_C\left(\sigma_{Ct+\frac{1}{2}\Delta t}, \varepsilon_{Ct+\frac{1}{2}\Delta t}^c\right), \quad (84)$$

where

$$\sigma_{Bt+\frac{1}{2}\Delta t} = \frac{E_B E_C}{E_B + E_C} \left(\varepsilon_{Ct+\frac{1}{2}\Delta t}^c - \varepsilon_{Bt+\frac{1}{2}\Delta t}^c + (\beta_C - \beta_B) m_{t+\frac{1}{2}\Delta t} \right), \quad (85)$$

$$\sigma_{Ct+\frac{1}{2}\Delta t} = \frac{E_B E_C}{E_B + E_C} \left(\varepsilon_{Bt+\frac{1}{2}\Delta t}^c - \varepsilon_{Ct+\frac{1}{2}\Delta t}^c + (\beta_B - \beta_C) m_{t+\frac{1}{2}\Delta t} \right), \quad (86)$$

with all material parameters evaluated for moisture content $m_{t+\frac{1}{2}\Delta t}$.

These non-linear equations for $\Delta\varepsilon_B^c$ and $\Delta\varepsilon_C^c$ can be solved using the Newton-Raphson method. The system of equations are rewritten as

$$F_B(\Delta\varepsilon_B^c, \Delta\varepsilon_C^c) = \frac{\Delta\varepsilon_B^c}{\Delta t} - f_B\left(\sigma_{Bt+\frac{1}{2}\Delta t}, \varepsilon_{Bt+\frac{1}{2}\Delta t}^c\right) = 0, \quad (87)$$

$$F_C(\Delta\varepsilon_B^c, \Delta\varepsilon_C^c) = \frac{\Delta\varepsilon_C^c}{\Delta t} - f_C\left(\sigma_{Ct+\frac{1}{2}\Delta t}, \varepsilon_{Ct+\frac{1}{2}\Delta t}^c\right) = 0, \quad (88)$$

and the solution is obtained by iterations using the formulas

$$\Delta \varepsilon_{Bn+1}^c = \Delta \varepsilon_{Bn}^c - \frac{F_B \frac{\partial F_C}{\partial \Delta \varepsilon_C^c} - \frac{\partial F_B}{\partial \Delta \varepsilon_C^c} F_C}{\frac{\partial F_B}{\partial \Delta \varepsilon_B^c} \frac{\partial F_C}{\partial \Delta \varepsilon_C^c} - \frac{\partial F_B}{\partial \Delta \varepsilon_C^c} \frac{\partial F_C}{\partial \Delta \varepsilon_B^c}} (\Delta \varepsilon_{Bn}^c, \Delta \varepsilon_{Cn}^c), \quad (89)$$

$$\Delta \varepsilon_{Cn+1}^c = \Delta \varepsilon_{Cn}^c - \frac{\frac{\partial F_B}{\partial \Delta \varepsilon_B^c} F_C - F_B \frac{\partial F_C}{\partial \Delta \varepsilon_B^c}}{\frac{\partial F_B}{\partial \Delta \varepsilon_B^c} \frac{\partial F_C}{\partial \Delta \varepsilon_C^c} - \frac{\partial F_B}{\partial \Delta \varepsilon_C^c} \frac{\partial F_C}{\partial \Delta \varepsilon_B^c}} (\Delta \varepsilon_{Bn}^c, \Delta \varepsilon_{Cn}^c), \quad (90)$$

where

$$\frac{\partial F_B}{\partial \Delta \varepsilon_B^c} = \frac{1}{\Delta t} + \frac{E_B E_C}{2(E_B + E_C)} \frac{\partial f_B}{\partial \sigma_B} - \frac{1}{2} \frac{\partial f_B}{\partial \varepsilon_B^c}, \quad (91)$$

$$\frac{\partial F_B}{\partial \Delta \varepsilon_C^c} = -\frac{E_B E_C}{2(E_B + E_C)} \frac{\partial f_B}{\partial \sigma_B}, \quad (92)$$

$$\frac{\partial F_C}{\partial \Delta \varepsilon_B^c} = -\frac{E_B E_C}{2(E_B + E_C)} \frac{\partial f_C}{\partial \sigma_C}, \quad (93)$$

$$\frac{\partial F_C}{\partial \Delta \varepsilon_C^c} = \frac{1}{\Delta t} + \frac{E_B E_C}{2(E_B + E_C)} \frac{\partial f_C}{\partial \sigma_C} - \frac{1}{2} \frac{\partial f_C}{\partial \varepsilon_C^c}. \quad (94)$$

A.2 The mechanical problem

From the solution to the pure moisture problem, the effective creep properties η_A , η_B , η_C , E_A^2 , E_B^2 and E_C^2 can be calculated according to Eqs (32–37).

The inner variables $\delta \varepsilon_A^c$, $\delta \varepsilon_B^c$ and $\delta \varepsilon_C^c$ and the stress $\delta \sigma^w$ must be updated. In finite element calculations it is preferred to use regular stresses $\delta \sigma$ instead of specific stresses $\delta \sigma^w$, so the following equations will be given for regular stresses, and the inner variables will change dimensions as appropriate. The relation between the different stresses is given by

$$\delta \sigma = \rho \rho_f \delta \sigma^w. \quad (95)$$

The inner stresses $\delta \sigma_A$, $\delta \sigma_B$ and $\delta \sigma_C$ are eliminated from Eqs (62–69) and Eq. (75), and the the remaining equations are rewritten as

$$k_A \Delta \delta \varepsilon_A^c = \delta \sigma_{At}^{\text{eff}} + \frac{\Delta \delta \sigma}{2}, \quad (96)$$

$$k_B \Delta \delta \varepsilon_B^c = \delta \sigma_{Bt}^{\text{eff}} + \frac{q_B \Delta \delta \sigma}{2} + \frac{k_{BC} (\Delta \delta \varepsilon_C^c - \Delta \delta \varepsilon_B^c)}{2} + \frac{\Delta k_{BC} (\delta \varepsilon_{Ct}^c - \delta \varepsilon_{Bt}^c)}{2}, \quad (97)$$

$$k_C \Delta \delta \varepsilon_C^c = \delta \sigma_{Ct}^{\text{eff}} + \frac{q_C \Delta \delta \sigma}{2} + \frac{k_{BC} (\Delta \delta \varepsilon_B^c - \Delta \delta \varepsilon_C^c)}{2}$$

$$+ \frac{\Delta k_{BC}(\delta \boldsymbol{\varepsilon}_{Bt}^c - \delta \boldsymbol{\varepsilon}_{Ct}^c)}{2}, \quad (98)$$

$$\begin{aligned} \Delta \delta \boldsymbol{\sigma} = & \mathbf{J} \Delta \delta \boldsymbol{\varepsilon} - \mathbf{K}_1 \Delta \delta \boldsymbol{\varepsilon}_A^c \\ & - q_B \mathbf{K}_2 \Delta \delta \boldsymbol{\varepsilon}_B^c - q_C \mathbf{K}_2 \Delta \delta \boldsymbol{\varepsilon}_C^c - \mathbf{K}_3 \delta \boldsymbol{\sigma}_t, \end{aligned} \quad (99)$$

where

$$k_A = \frac{E_A^2}{2} + \frac{\eta_A}{\Delta t}, \quad (100)$$

$$k_B = \frac{E_B^2}{2} + \frac{\eta_B}{\Delta t}, \quad (101)$$

$$k_C = \frac{E_C^2}{2} + \frac{\eta_C}{\Delta t}, \quad (102)$$

$$k_{BC} = \frac{E_B E_C}{E_B + E_C}, \quad (103)$$

$$q_B = \frac{E_B}{E_B + E_C}, \quad (104)$$

$$q_C = \frac{E_C}{E_B + E_C}, \quad (105)$$

$$\delta \boldsymbol{\sigma}_{At}^{\text{eff}} = \delta \boldsymbol{\sigma}_{At} - E_A^2 \delta \boldsymbol{\varepsilon}_{At}^c, \quad (106)$$

$$\delta \boldsymbol{\sigma}_{Bt}^{\text{eff}} = \delta \boldsymbol{\sigma}_{Bt} - E_B^2 \delta \boldsymbol{\varepsilon}_{Bt}^c, \quad (107)$$

$$\delta \boldsymbol{\sigma}_{Ct}^{\text{eff}} = \delta \boldsymbol{\sigma}_{Ct} - E_C^2 \delta \boldsymbol{\varepsilon}_{Ct}^c, \quad (108)$$

$$\mathbf{J} = \rho \mathbf{C} \left(\frac{\mathbf{L}}{E_A} + \frac{\mathbf{C} - \mathbf{L}}{E_B + E_C} \right)^{-1} \mathbf{C}, \quad (109)$$

$$\mathbf{K}_1 = \mathbf{C} \left(\frac{\mathbf{L}}{E_A} + \frac{\mathbf{C} - \mathbf{L}}{E_B + E_C} \right)^{-1} \mathbf{L} \mathbf{C}^{-1}, \quad (110)$$

$$\mathbf{K}_2 = \mathbf{C} \left(\frac{\mathbf{L}}{E_A} + \frac{\mathbf{C} - \mathbf{L}}{E_B + E_C} \right)^{-1} (\mathbf{C} - \mathbf{L}) \mathbf{C}^{-1}, \quad (111)$$

$$\mathbf{K}_3 = \mathbf{C} \left(\frac{\mathbf{L}}{E_A} + \frac{\mathbf{C} - \mathbf{L}}{E_B + E_C} \right)^{-1} \Delta \left(\frac{\mathbf{L}}{E_A} + \frac{\mathbf{C} - \mathbf{L}}{E_B + E_C} \right) \mathbf{C}^{-1}. \quad (112)$$

It is assumed that the elastic moduli E_B and E_C have similar dependencies on moisture content, so that q_B and q_C do not depend on moisture content. All other parameters must be evaluated at moisture content $m_{t+\frac{1}{2}\Delta t}$. If the moisture content changes during the increment, there will be a contribution to the equations from the changing material parameters. These contributions are found in Eqs (97–98) and Eq. (112), where Δ before an expression denote an incremental change of that expression.

\mathbf{J} in Eq. (109) is the material Jacobian that must be provided by the material subroutine in ABAQUS (2002), i.e.

$$\frac{\partial \Delta \delta \boldsymbol{\sigma}}{\partial \Delta \delta \boldsymbol{\varepsilon}} = \mathbf{J} = \rho \mathbf{C} \left(\frac{\mathbf{L}}{E_A} + \frac{\mathbf{C} - \mathbf{L}}{E_B + E_C} \right)^{-1} \mathbf{C}. \quad (113)$$

Eqs (96–99) constitute a system of linear equations, that can easily be solved. The stress increment $\Delta \delta \boldsymbol{\sigma}$ is given by

$$\begin{aligned} \Delta \delta \boldsymbol{\sigma} = & \left(\mathbf{I} + \frac{\mathbf{K}_1}{2k_A} + \frac{(2q_B^2 k_C + 2q_C^2 k_B + k_{BC}) \mathbf{K}_2}{2(2k_B k_C + (k_B + k_C) k_{BC})} \right)^{-1} \\ & \left(\mathbf{J} \Delta \delta \boldsymbol{\varepsilon} - \frac{\mathbf{K}_1 \delta \boldsymbol{\sigma}_{At}^{\text{eff}}}{k_A} \right. \\ & \quad - \frac{(2q_B k_C + k_{BC}) \mathbf{K}_2 \delta \boldsymbol{\sigma}_{Bt}^{\text{eff}}}{2k_B k_C + (k_B + k_C) k_{BC}} \\ & \quad - \frac{(2q_C k_B + k_{BC}) \mathbf{K}_2 \delta \boldsymbol{\sigma}_{Ct}^{\text{eff}}}{2k_B k_C + (k_B + k_C) k_{BC}} \\ & \quad \left. - \frac{(q_B k_C - q_C k_B) \Delta k_{BC} \mathbf{K}_2 (\delta \boldsymbol{\varepsilon}_{Ct}^c - \delta \boldsymbol{\varepsilon}_{Bt}^c)}{2k_B k_C + (k_B + k_C) k_{BC}} \right. \\ & \quad \left. - \mathbf{K}_3 \delta \boldsymbol{\sigma}_t \right). \end{aligned} \quad (114)$$

The increments of the inner variables are

$$\Delta \delta \boldsymbol{\varepsilon}_A^c = \frac{\delta \boldsymbol{\sigma}_{At}^{\text{eff}}}{k_A} + \frac{\Delta \delta \boldsymbol{\sigma}}{2k_A}, \quad (115)$$

$$\begin{aligned} \Delta \delta \boldsymbol{\varepsilon}_B^c = & \frac{(2k_C + k_{BC}) \delta \boldsymbol{\sigma}_{Bt}^{\text{eff}} + k_{BC} \delta \boldsymbol{\sigma}_{Ct}^{\text{eff}} + k_C \Delta k_{BC} (\delta \boldsymbol{\varepsilon}_{Ct}^c - \delta \boldsymbol{\varepsilon}_{Bt}^c)}{2k_B k_C + (k_B + k_C) k_{BC}} \\ & + \frac{(2q_B k_C + k_{BC}) \Delta \delta \boldsymbol{\sigma}}{2(2k_B k_C + (k_B + k_C) k_{BC})}, \end{aligned} \quad (116)$$

$$\begin{aligned} \Delta \delta \boldsymbol{\varepsilon}_C^c = & \frac{k_{BC} \delta \boldsymbol{\sigma}_{Bt}^{\text{eff}} + (2k_B + k_{BC}) \delta \boldsymbol{\sigma}_{Ct}^{\text{eff}} + k_B \Delta k_{BC} (\delta \boldsymbol{\varepsilon}_{Bt}^c - \delta \boldsymbol{\varepsilon}_{Ct}^c)}{2k_B k_C + (k_B + k_C) k_{BC}} \\ & + \frac{(2q_C k_B + k_{BC}) \Delta \delta \boldsymbol{\sigma}}{2(2k_B k_C + (k_B + k_C) k_{BC})} \end{aligned} \quad (117)$$

with $\Delta \delta \boldsymbol{\sigma}$ according to Eq. (114).

References

- ABAQUS (2002). *ABAQUS User's manual Version 6.3*. Hibbitt, Karlsson & Sorensen, Inc., Pawtucket, Rhode Island.
- Alfthan, J. (2003). A simplified network model for mechano-sorptive creep in paper. *J. Pulp Paper Sci.*, 29(7):228–234.
- Alfthan, J., Gudmundson, P., and Östlund, S. (2002). A micro-mechanical model for mechano-sorptive creep in paper. *J. Pulp Paper Sci.*, 28(3):98–104.
- Armstrong, L. D. and Christensen, G. N. (1961). Influence of moisture changes on deformation of wood under stress. *Nature*, 191(4791):869–870.
- Armstrong, L. D. and Kingston, R. S. T. (1960). Effect of moisture changes on creep in wood. *Nature*, 185(4718):862–863.
- Byrd, V. L. (1972a). Effect of relative humidity changes during creep on handsheet paper properties. *Tappi*, 55(2):247–252.
- Byrd, V. L. (1972b). Effect of relative humidity changes on compressive creep response of paper. *Tappi*, 55(11):1612–1613.
- Coffin, D. W. and Habeger, C. C. (2001). The mechanics of sorption-induced transients in the loss tangent. *J. Pulp Paper Sci.*, 27(11):385–390.
- Habeger, C. C. and Coffin, D. W. (2000). The role of stress concentrations in accelerated creep and sorption-induced physical aging. *J. Pulp Paper Sci.*, 26(4):145–157.
- Habeger, C. C., Coffin, D. W., and Hojjatie, B. (2001). Influence of humidity cycling parameters on the moisture-accelerated creep of polymeric fibers. *J. Polym. Sci. Part B Polym. Phys.*, 39(17):2048–2062.
- Komori, T. and Makishima, K. (1977). Numbers of fiber-to-fiber contacts in general fiber assemblies. *Text. Res. J.*, 47(1):13–17.
- MATLAB (2001). *MATLAB 6.1*. The MathWorks, Inc, Natick, Massachusetts.
- Panek, J., Fellers, C., and Haraldsson, T. (2004). Principles of evaluation for the creep of paperboard in constant and cyclic humidity. *Nord. Pulp Pap. Res. J.*, 19(2):155–163.
- Pickett, G. (1942). The effect of change in moisture-content of the creep of concrete under a sustained load. *J. Amer. Concrete Inst.*, 13(4):333–355.

- Wang, J. Z., Davé, V., Glasser, W., and Dillard, D. A. (1993). The effects of moisture sorption on the creep behavior of fibers and composite materials. In Harris, C. and Gates, T., editors, *High Temperature and Environmental Effects on Polymeric Composites*, volume 1174 of *ASTM STP*, pages 186–200. ASTM.
- Wang, J. Z., Dillard, D. A., and Kamke, F. A. (1991). Transient moisture effects in materials. *J. Mat. Sci.*, 26:5113–5126.
- Wang, J. Z., Dillard, D. A., and Ward, T. C. (1992). Temperature and stress effect on the creep of aramid fibers under transient moisture conditions and discussions on the mechanism. *J. Polym. Sci. Part B Polym. Phys.*, 30:1391–1400.
- Wang, J. Z., Dillard, D. A., Wolcott, M. P., Kamke, F. A., and Wilkes, G. L. (1990). Transient moisture effect in fibers and composite materials. *J. Compos. Mater.*, 24:994–1009.